INL/CON-19-53593
PREPRINT

Rate/Concentration Kinetic Petals: A Transient Method to Examine the Interplay of Surface Reaction Processes

Journal of Physical Chemistry A

Yixiao Wang, M. Ross Kunz,
Denis Constales, Gregory Yablonsky,
Rebecca Fushimi

September 2019

The INL is a
U.S. Department of Energy
National Laboratory
operated by
Battelle Energy Alliance

Rate/Concentration Kinetic Petals: A Transient Method to Examine the Interplay of Surface Reaction Processes

Yixiao Wang[1], M. Ross Kunz[1], Denis Constales[2], Gregory Yablonsky[3], Rebecca Fushimi[1*]

[1]Idaho National Laboratory, Idaho Falls, ID, USA
[2]Ghent University, Ghent 9000, Belgium
[3]Washington University in St. Louis, St. Louis, MO, USA
**Corresponding Author: rebecca.fushimi@inl.gov*

ABSTRACT

Transient pulse response experiments are used to construct rate/concentration (RC) kinetic dependencies—RC petals—and provide a new method to distinguish the timing and interplay of adsorption, surface reaction, and product formation on complex (industrial) materials. A petal shape arises as the dynamic "reaction-diffusion" experiment forces the concentration and reaction rate to return to zero. In contrast to the typical steady-state "Langmuir-type" RC dependence, RC petals have two branches, which arise as a result of decoupled gas and surface concentrations in the non-steady-state regime. To demonstrate this approach, the characteristics of petal shapes using ammonia decomposition as a probe reaction are presented. Ammonia, hydrogen, and nitrogen transformation rates are compared on three simple materials: Fe, Co, and a bimetallic CoFe preparation when ammonia is pulsed at 550°C in a low-pressure diffusion reactor. All materials demonstrate a two-branch kinetic RC dependence for ammonia adsorption, and rate constants are quantified in the low-coverage regime. We found that H_2 and N_2 product formation was dependent on the concentration of surface intermediates for all materials with one exception: for Co, an additional fast hydrogen generation process was observed; the rate of which coincided with ammonia adsorption. Nitrogen generation was only significant for CoFe and Co and on the CoFe catalyst, a self-inhibition property was observed. A method for estimating the number of active sites based on the RC petals is presented and was applied to the Fe and CoFe samples. The surface coverage and rate of formation/conversion of surface intermediates are interpreted from the examination of shape characteristics of the RC petals for each material.

GRAPHICAL ABSTRACT

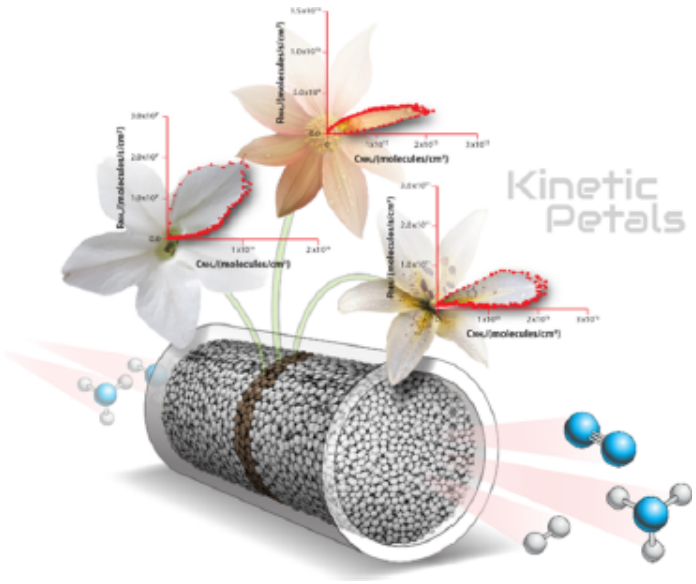

1. INTRODUCTION

The dependence of the chemical transformation rate on the concentration of gas-phase species is essential information for kinetic modeling and characterization of a heterogeneous catalyst. The continuous stirred tank reactor (CSTR) and plug flow reactor (PFR) are the most commonly used tools for generating rate/concentration (RC) data at steady-state conditions. Kinetic models of most industrial catalytic processes are based upon this type of data. Typically, these dependencies are described as a "Langmuir-type" relationship, as depicted in Figure 1. For a gas-solid catalytic reaction under steady-state conditions, the kinetic dependence is presented as:

$$R = f\,(k(T),\, C,\, N_{\mathrm{m}}) \tag{1}$$

where k is a set of kinetic parameters, T is an absolute temperature, C is a set of gas-phase concentrations, and N_m is a set of catalyst characteristics (bulk or surface) that do not change during a kinetic characterization experiment (e.g., the number of surface metal atoms or surface intermediates). At the steady-state, the concentrations of surface species are dependent on the gas-phase concentrations.

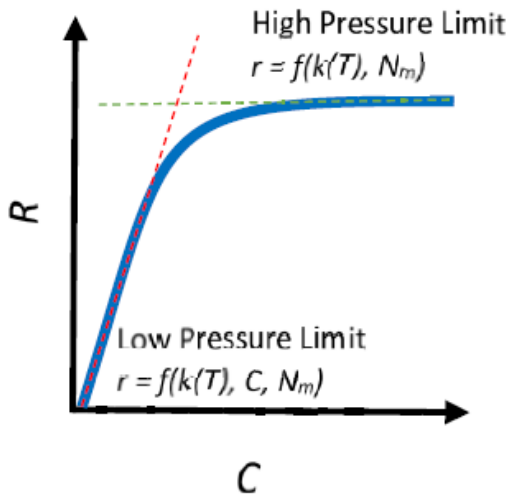

Figure 1. Typical steady-state CSTR rate/concentration dependence.

The steady-state RC kinetic dependence can be analyzed using the Langmuir-Hinshelwood-Hougen-Watson (LHHW) method [1–4]. Hinshelwood developed the method based on the Langmuir adsorption isotherm [5,6]. A similar approach was later developed by Hougen and Watson that popularized the Langmuir-Hinshelwood kinetics [7]. In a typical steady-state kinetic dependence, two characteristics can be determined:

(a) the initial slope that determines the initial apparent kinetic constant

(b) the plateau ("the reaction rate limit") in which active sites are mostly occupied.

The advantage of this LHHW method (e.g., in comparison to the empirical power-law approach) is that adsorption/desorption processes and surface reactions are considered. The rate equation is derived in terms of surface concentration of adsorbed species and vacant sites. Then, these surface concentrations are related to the gas concentrations that can be directly measured. For example, for ammonia decomposition, using the Langmuir-Hinshelwood description of uniform adsorption and maintaining all adsorbed species as kinetically relevant, detailed development of rate expressions using this method was presented by Armenise et al. [8].

The overall rate expression can be greatly simplified by assuming that one slow step controls the overall rate and remaining steps are near equilibrium. For example, for ammonia synthesis, the following rate expression was derived by Stoltze and Norskov, assuming that the rate of nitrogen dissociation is limiting [9]

$$r = k_2^+ K_1 P_{N_2} \theta_*^2 - k_2^- \left[\frac{P_{NH_3}}{K_3 K_4 K_5 K_6 (K_7 P_{H_2})^{3/2}} \right]^2 \theta_*^2 \quad (2)$$

Further simplifications can then be made by evaluating equilibrium conditions (e.g., $K_G =$ $=$; $=$). Parameter values may be obtained by fitting experimental data using optimum search methods. For example, experimental ammonia synthesis data fitted to the model described in Eq. 2 demonstrates god agreement over a wide range of conditions (357–500°C,
1–300 atm) [9]. Many microkinetic parameters may be determined from surface science and computational studies. Data collected from nonequilibrium surface science conditions are generally represented by much simpler rate expressions as reverse reactions from the gas phase can be neglected.

In this work, we present rate/concentration dependencies derived from unique non-steady-state experimental conditions using the temporal analysis of products (TAP) pulse response technique [10,11]. The general RC dependence for the non-steady state can be presented as follows

(3)

In contrast to the steady-state, Eq. 1 and Eq. 5 include θ, which represents a set of independent non-steady-state surface concentrations. No assumptions about their equilibrium and/or quasi-steady-state behavior are formulated. Therefore, surface concentrations are not considered to be functions of the gas concentration as in the steady-state experiment. The non-steady-state experiment, thus, reflects the detailed mechanistic complexity of changing surface concentrations on the catalytic reaction. In this case, the RC kinetic dependence will be a projection of Eq. 5 in the R-C plane.

In the TAP pulse response method, the primary experimental data is exit flux. This is not pure kinetic data as it contains both kinetic and transport phenomena at the exit of the reactor. To extract pure kinetic data in the active zone of the reactor, the Y-Procedure analytical method can be utilized to transform the exit flux data into the temporal rate and concentration data [12,13]. This analysis decouples chemical kinetics and diffusional transport using an "inverse-diffusion" method in the Laplace domain to translate the flux forward/backward from the entrance/exit of the reactor to the catalyst zone. In a typical steady-state catalytic experiment, the reactant concentration is fixed, consequently, only one set of surface coverages and one apparent rate constant can be determined. By observing the catalyst response to a pulse, the TAP technique explores a range of reactant concentrations, surface coverages, and rate constants. As a result, the extent of kinetic data that can be accessed is significantly greater than with steady-state conditions; a feature which opens the door to machine learning and data science tools (a topic that will be addressed separately).

The rate/concentration dependence derived from pulse response experiments is described here as RC petals using experimental pulse response data of ammonia decomposition over Fe, Co, and a bimetallic preparation of the two. A petal shape arises when the dynamic experiment forces the concentration and rate to return to zero. In the theory of dynamic processes, "variable-variable" or "derivative-variable" dependences are described as phase portraits. Therefore, the petal can be defined mathematically as a phase trajectory; in particular, a closed-loop trajectory.

RC petals have, hereto now, only been described using simulation and experimental data from the oxidation of platinum [12–14] and CO adsorption/oxidation on platinum [15,16].

In a previous publication [17], we described the structural properties of the ammonia decomposition materials in greater detail along with the time dependence of the transformation rate of ammonia together with hydrogen and nitrogen products. The time dependence of the transformation rate taken together with the gas-phase concentration data, the RC petal, reveals a changing apparent rate constant that indicates the role of surface species in the reaction process. In the presentation of general petal concepts, we provide a mathematical basis to utilize the rate time dependence to estimate the number of active sites. RC petals from ammonia decomposition experiments presented unique features for the Fe, Co, and bimetallic materials. The discussion of these features demonstrates the RC petal concept as a "kinetic fingerprint" for comparing fundamental performance across a set of materials at well-defined conditions.

2. EXPERIMENT AND METHODS

2.1 Catalyst Preparation and Structural Characterization

Three materials were compared: polycrystalline Fe (99.99% purity, particle size 450 μm, Goodfellow), polycrystalline Co (99.9% purity, particle size 600 μm, Alfa Aesar), and a bimetallic CoFe preparation. Polycrystalline Fe and Co were sieved to the 250−300 μm particle size range. The bimetallic sample was prepared by wet impregnation of Co(II) nitrate hexahydrate, $Co(NO_3)2{\cdot}6H_2O$ (99.999% purity, Sigma Aldrich) onto the polycrystalline Fe sample. Nominally, 1 ML of Co was deposited over the Fe support. These materials were characterized more thoroughly in a previous publication [17].

2.2 TAP Pulse Response Experiments and Analysis

CoFe and Co samples were reduced with 10% H_2/Ar flow at 550°C for about 17 h before loading in the TAP reactor with a thin-zone configuration [18] for titration experiments. Samples were exposed to ambient upon loading but were again reduced, *in situ*, with the same 10% H_2/Ar flow at 550°C overnight. Ammonia pulse response data were collected at 550°C with a collection time of 3 s and a pulse spacing of 3.3 s. A 50 vol%NH_3 in Ar (UHP, 99.999%, Matheson Gas) was used, and AMUs 17, 2, 28, and 40 were monitored in sequence to track ammonia, hydrogen, nitrogen, and argon. More details of the experimental procedure can be found in a previous publication [17].

The experimental pulse response data of reactants and products were preprocessed prior to the application of the Y-Procedure to calculate reaction rates, details were provided previously [14,17]. Briefly, this included calibration and scaling of gas flux over an inert reactor bed at 550°C followed by baseline correction of the last 0.5 s of the flux. The reaction rate and gas concentration were calculated according to the Y-Procedure [12–14]. The diffusion of hydrogen and nitrogen was calculated by scaling the argon pulse according to Graham's law. For ammonia, the pulse response collected over inert bed experiments was used to account for transport since a minor adsorption/desorption is observed between silica and ammonia at 550°C.

3. RESULTS AND DISCUSSION

3.1 Catalyst Textural Properties and Composition

Measured by inductively coupled plasma optical emission spectrometry, the mass loading of Co on the bimetallic sample was 3.16 wt %. The Brunauer-Emmett-Teller surface areas of Fe and CoFe were both 4.5m^2/g and it was 1m^2/g for Co. CoFe showed general spherical morphology and an average crystallite size of 94 nm with a uniform distribution of Co throughout the whole of the Fe surface. More detailed characterization results can be found in the work by Wang et al. [17].

3.2 Gas Concentration Time Dependence

The concentration time dependence calculated for reactants and products over all samples can be found in the *Supporting Information*. The concentration time dependence is more informative when it is considered in conjunction with the rate data, as will be described in Section 3.4. In the discussion of this feature, it should be noted that for precise kinetic characterization, one of the most important tasks is to properly account for reactor transport in rate/concentration data. The TAP exit flux contains information about both transport and kinetics, but the desired information is a concentration in the catalyst zone and the responding transformation rate. The Y-Procedure methodology provides this information by decoupling the timing of diffusional transport in the inert zones so that the concentration time dependence solely reflects the kinetic process taking place in the catalyst zone. Similarly, the thin-zone reactor configuration physically decouples transport and kinetics. In a differential PFR at low conversion, the change in the concentration across the catalyst bed is assumed to be insignificant and an average concentration is often used [4,19] Similarly, the concentration change across the thin-zone TAP reactor is assumed to be insignificant, and with diffusion acting as an efficient "impeller," the thin-zone is well-mixed. Although the rate in a PFR is a difference of concentrations, in TAP, the rate is a difference in concentration gradients (or fluxes); thus, kinetic data can be evaluated at much higher conversions [17, 20].

3.3 Reaction Rate Time Dependence

In NH_3-pulsed experiments over the Fe, CoFe, and Co samples at 550°C, reactant conversions of 10 ± 2, 90 ± 2, and 85 ± 2% were observed, respectively [17]. N_2 and H_2 were the only gas-phase products detected. The reaction rates calculated using the Y-Procedure for reactants and products are presented in Figure 2; rates are height-normalized for comparison of time characteristics. Note that according to the Y-Procedure, the rate is calculated from a difference in fluxes into and out of the catalyst thin zone; it is not a result of numerical differentiation.

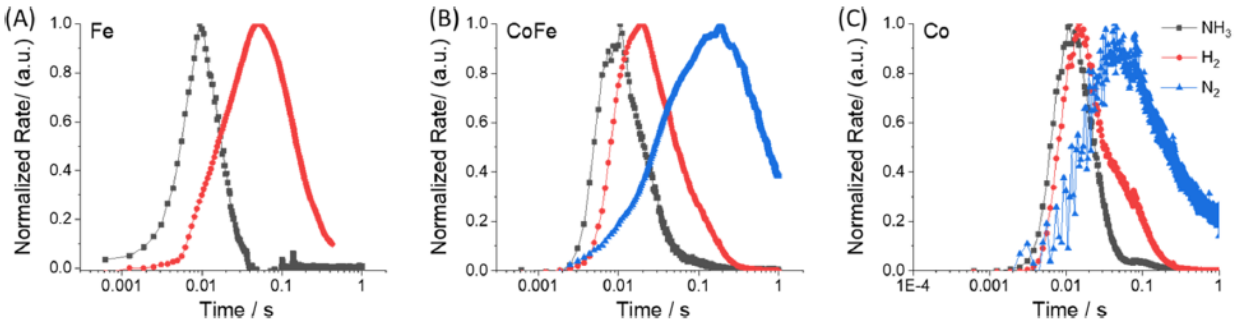

Figure 2. Time dependence of the reaction rate determined for NH_3 and products (H_2 and N_2) when NH_3 is pulsed over Fe, CoFe, and Co at 550°C. Data has been height-normalized for comparison of time characteristics.

In all of the cases, the maximum in the rate of ammonia conversion precedes the maximum in product generation. Nitrogen generation over the Fe sample was too low for rate analysis; however, a significant delay between the conversion of ammonia and generation of hydrogen was observed. This delay decreases over the CoFe sample, and the onset of hydrogen production is in close correspondence to ammonia conversion over the Co sample. For both CoFe and Co, the generation of nitrogen follows that of hydrogen. The difference between the timing for ammonia conversion and generation of products is an indication of the timing of surface processes.

3.4 Primary Rate/Concentration Petal Concepts

The experimentally observed exit flux was used to calculate the time dependence of the rate and concentration (*Supporting Information*) via the Y-Procedure method, as shown in Figure 3. The diffusional transport is a "driving force," which increases the gas concentration with the pulse injection and likewise decreases it as the pulse escapes the reactor. The dynamic experiment, thus, forces the gas concentration and hence transformation rate to return to zero; this creates a petal shape when the time dependence of each is evaluated together, as can be seen in Figure 3C. A rate/concentration (RC) dependence provides primary information needed for understanding how a chemical transformation takes place on an active surface. Active sites respond to a reactant gas mixture by generating products at a rate dependent on the surface coverage and temperature. As such, when decoupled from transport information, the RC dependence is an intrinsic characterization of the state of the catalyst surface and is useful for benchmark comparison of different materials and catalyst states (e.g., surface coverage, composition, structure, etc.). As the transient experiment evaluates the transformation rate over a range of gas and surface coverages in each measurement, it can be considered a high-throughput kinetic device in comparison to conventional steady-state measurements.

In this work, we will only consider the case for a global irreversible gas/solid reaction. The following features of the RC petal are important in the analysis:

- the petal width, branches, and directionality
- the rate maximum and concentration maximum.

The width of the RC petal is a qualitative characteristic of the catalyst composition change during the experiment. A narrow petal, approximated by a straight line, indicates insignificant change, a "state-defining" experiment, while a wide petal indicates a significant change in the catalyst composition, a "state-altering" experiment (see references [12,21,22] for a greater discussion on state-defining and state-altering experiments). In Figure 3C, two branches of the petal, ascending and descending regarding concentration, are characterized by the increase and decrease of the gas concentration during the pulse. Also identified are points *O*, *A*, and *B* indicating the origin and maximum in the rate and concentration,

respectively. The segment , which includes the rate maximum, *A*, represents the ascending branch, while the segment from the concentration maximum to the origin represents the descending branch. Within the domain , both rate and concentration are increasing. Within the domain , the rate may remain constant or decrease, while the concentration continues to increase. The domain is decreasing with respect to both rate and concentration.

The two-branch petal is characterized by two values of the reaction rate at any given gas concentration and, likewise, with two values of concentration at any reaction rate. This is the key difference between the state-altering RC dependence in the pulse regime and the typical Langmuir-type RC dependence for the steady-state regime where only one reaction rate is observed at a given gas concentration. In state-altering petals, a plateau may be identified near the reaction rate maximum and, likewise, a "cliff" can be observed near the concentration maximum.

In a "gas-solid" interaction, the slope of the ascending branch represents the apparent rate constant, which includes the number of free active sites: . The surface is partially covered by the corresponding intermediate, and the number of free active sites decreases. The effect is compensated by the rise in the gas concentration and the reaction rate may exhibit a plateau (a Langmuir-type dependence). The effective of free active sites diminishing may become more significant, and the reaction rate can begin to decrease within the domain of . In this region, the rate may decline or extinguish (indicating that free active sites have been exhausted). A decline in this region, prior to the concentration maximum, indicates that the rate of reactant adsorption is inhibited by accumulated surface species. Following the concentration maximum, the gas-phase concentration begins to decrease mostly represents physical transport phenomena.

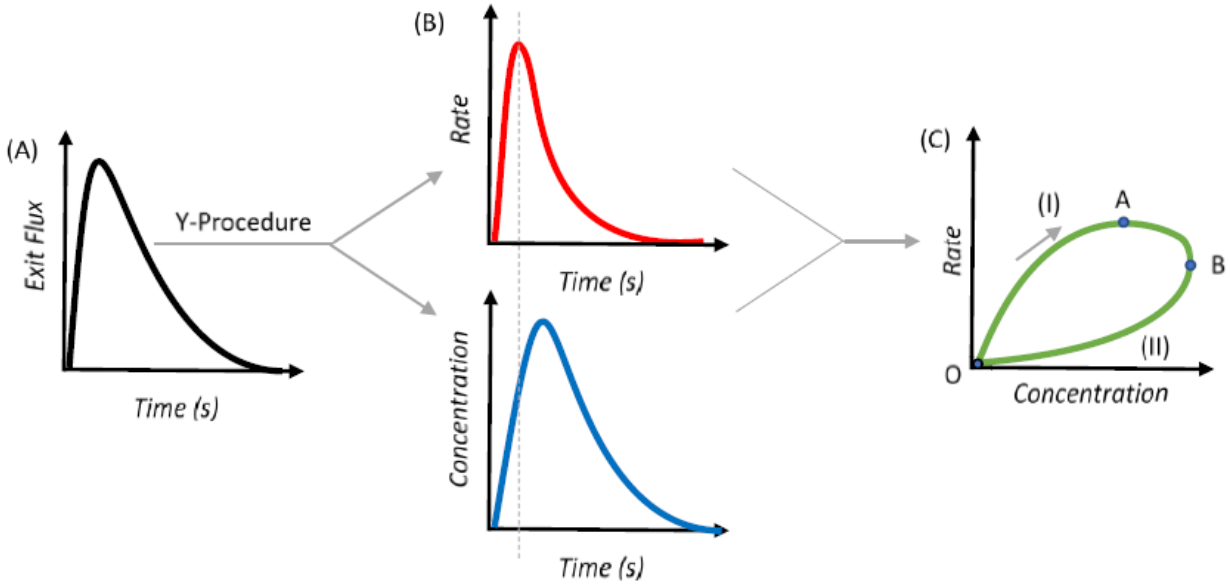

Figure 3. (A) Exit flux is the experimental observable in the TAP pulse response experiment. The Y-Procedure method is used to calculate the time dependence of (B) the rate and gas concentration in the active catalyst zone. A plot of rate versus concentration (C) always returns to zero in the dynamic experiment forming a characteristic RC petal. Characteristic regions of the RC petal are identified in (C): (I) ascending branch, and (II) descending branch along with the origin labeled O, as well as points A and B, which represent the rate and concentration maxima, respectively.

Generally, it makes sense to distinguish the following types of petals:

(a) Reactant rate versus reactant concentration.

(b) Product rate versus reactant concentration.

(c) Reactant rate versus product concentration.

(d) Product rate versus product concentration.

In this work, we will not analyze cases (c) and (d) under the assumption that backward reactions from our products (e.g., nitrogen and hydrogen) do not significantly impact the forward reaction rates due to our experimental conditions. Each petal is characterized by a directionality. In case (a), adsorption of the reactant decreases the concentration of free active sites; the apparent kinetic constant (slope of the RC petal) decreases as well; the petal is then formed in a clockwise fashion. For products in case (b), the interplay of adsorption, formation of surface intermediates, and the release of products will determine the directionality. A clockwise trend indicates that product formation is primarily dependent on the concentration of the reactant. Three cases can be considered:

(i) product is generated via the direct interaction of the reactant with the catalyst, ; where and are reactant and product, respectively. and are the active center and surface intermediate, respectively.

(ii) a two-step reaction where the conversion of the reactant to the surface intermediate is fast and reversible, (*or*); where and are corresponding intermediates.

(iii) a two-step reaction where the conversion of the surface intermediate to the product is faster than the reactant to the surface intermediate, (*or*).

In case (i), the product is directly formed in the first step of the reactant interacting with the catalyst. In case (ii), it is easy to show that the second step is under quasi-equilibrium and the surface intermediate is proportional to the gas concentration of the reactant. Consequently, the rate of formation of the product will be proportional to the concentration of the reactant. In case (iii), the surface intermediate is highly reactive and the surface concentration will be low, can be viewed as a quasi-steady-state species.

A counterclockwise trend in RC petals for case (b) indicates that the product generation does not occur via direct interaction of the reactant with the catalyst and that some transformation steps through surface species are involved. This trend will be observed when the product is formed from some intermediate that is not equilibrated with respect to the gaseous reactant or offset by fast consumption. In this case, the transformation of the surface intermediate to the product must be the slow step; (*or*). Therefore, we need to interpret such counterclockwise dependencies in terms of product rate as a function of surface concentration instead. At the present level of analysis, such statements on counterclockwise versus clockwise petals are not rigorous but more qualitative. However, they can be used for the primary recognition of mechanistic details. The quantitative analysis of clockwise and counterclockwise kinetic petals will be addressed in a separate paper.

3.5 Experimental Ammonia Decomposition Rate/Concentration Petals

In this example, we consider that the conversion of ammonia is irreversible (i.e., products, hydrogen, and nitrogen do not readsorb to form ammonia over the catalyst). In Figure 4, we present the RC petals for the rate of transformation of ammonia production of hydrogen and nitrogen as a function of the ammonia gas concentration over the Fe, bimetallic, and Co catalyst. Petals are not presented as a function of the product concentration since the readsorption of the product is negligible. A summary of findings for primary petal concepts is found in Table 1.

Table 1. Summary of primary petal concepts derived from experimental ammonia decomposition data.

	Fe	**CoFe**	**Co**
		Ammonia	
shape	asymmetric	symmetric	asymmetric
width	wide (state-altering)	wide (state-altering)	wide (state-altering)
maxima			

direction	clockwise	clockwise	clockwise
		Hydrogen	
shape	asymmetric	symmetric	asymmetric
width	wide (state-altering)	narrow (state-altering)	wide (state-altering)
maxima			
direction	counterclockwise	counterclockwise	counterclockwise
		Nitrogen	
shape		asymmetric	asymmetric
width		wide (state-altering)	wide (state-altering)
maxima			
direction		counterclockwise	counterclockwise

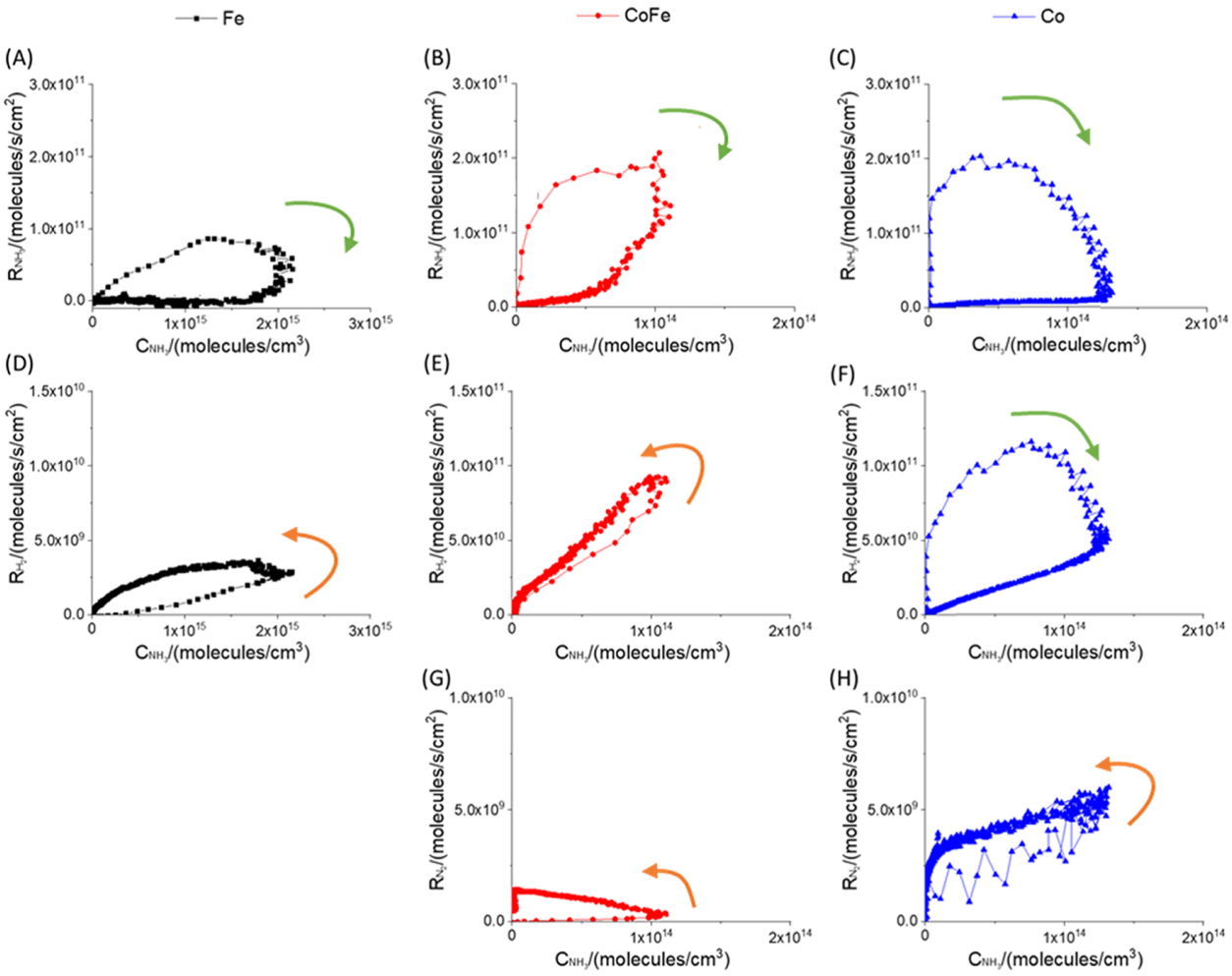

Figure 4. (A)-(C) Rate/Concentration (RC) petals for ammonia, (D)-(F) hydrogen RC petals, (G) and (H) nitrogen RC petals when ammonia is pulsed over Fe, CoFe, and Co catalysts at 550°C. All rates are plotted as functions of ammonia concentration. Arrows indicate directionality of the petal (in general, this can be identified with the density of data points, the change is the greatest early in the experiment and

sparsity of points is greater).

3.5.1 Ammonia Reactant RC Petals

Figure 4A and Figure 4C show a dynamic change of the ammonia transformation rate as a function of the gas-phase concentration when pulsed at 550°C over Fe, CoFe, and Co samples, respectively. The ammonia RC petal shape for CoFe, as shown in Figure 4B, demonstrates most clearly that at a singular gas concentration, two different reaction rates can be observed, and, hence, the surface coverage changes significantly during the pulse. Though the ammonia rate is on the same order of magnitude for all samples, the gas concentration scale for the CoFe and Co catalysts is roughly 10x less than that of Fe. This is due to the much higher conversion observed on materials with Co.

The slope of the ascending branch represents the apparent rate constant. An increase in the apparent rate constant[a] is observed from 4.8 × 107/s, 4.2 × 109/s, and 3.5 × 1010/s for Fe, CoFe, and Co, respectively. The number of free active sites decreases as uptake proceeds and the surface becomes covered by surface intermediates. In Figure 4A, on the ascending branch, the rate is observed to assume a general plateau (perhaps slightly declining) before the concentration maximum is reached. This indicates that the surface concentration has a greater effect than the gas concentration. The rate becomes limited due to the decreasing availability of free sites. Near the concentration maximum, for the Fe sample, we observe the rate to drop rapidly at a single value of the gas concentration. Here, the rate must be controlled by the surface coverage. The rate is then extinguished, as the pulse exits the reactor.

In Figure 4B, we observe that the maximum in the rate coincides with the maximum in gas concentration on the CoFe sample. The rate is observed to slow with accumulating surface species and does not decline until the concentration maximum. Similar to Fe, the rate quickly drops at the concentration maximum but is not as rapidly extinguished. The petal shape for CoFe is symmetrical, while that of Fe is not. In this case, the reaction rate reverses and follows the pulse response; it is not extinguished due to limited free sites as in the case of Fe. To understand this, comparison of the timing of the rate distribution and the magnitude of rates is helpful. In Figure 2, the timing of reactant/product rates shows greater overlap for CoFe than Fe. The magnitudes of the rates of hydrogen formation and ammonia conversion are similar on CoFe, there is a >10-fold imbalance on Fe. Thus, for Fe, the ammonia rate is extinguished, while for CoFe, the release of hydrogen and nitrogen may free active sites for the conversion of ammonia molecules arriving late in the pulse.

The Co sample in Figure 4C shows similar Langmuir-type behavior as the CoFe sample on the ascending branch and into the transition region. Following the plateau, however, the rate decreases even as the gas concentration is still increasing. From one point of view, this indicates that although sites are still available, the rate has become inhibited by accumulating surface species. Once sites are irreversibly consumed, the rate will extinguish. However, if another process regenerates free sites (e.g., the production of gas-phase H_2 and N_2, then the rate may continue). In this case, sites are quickly consumed before the concentration maximum is reached and the regeneration of free sites leads to a slower decline in the rate. At the turning point, the rate is negligible, but the gas concentration is still high. This indicates that active sites are no longer available.

3.5.2 Hydrogen and Nitrogen Product RC Petals

The adsorption rate of the reactant is clearly affected by the coverage of surface species, as demonstrated in the transition region of the ammonia RC petals for each catalyst. Although the conversion of the reactant increases surface coverage, we also need to consider the regeneration of active sites, as products are formed and released. Figure 4D and Figure 4F show the RC petals for hydrogen—and Figure 4G and Figure 4H for nitrogen—that formed during the ammonia pulse over each catalyst. The rate of product formation is plotted with respect to the reactant gas-phase concentration. For

[a]Taken directly from the R/C plot, the units of the rate constant are (cm/s), here we have taken surface area, bed volume, and voidage to give units of (1/s).

products, the interplay of multiple surface reaction processes may result in nonlinear RC dependences and the RC petals are significantly different (e.g., width and direction).

3.5.2.1 *Fe Sample*

The overall conversion of ammonia was significantly lower on Fe and likewise the rate of hydrogen formation, Figure 4D (note that the scale is different from hydrogen production on the other samples). In accordance with our preliminary considerations, two steps can be considered: first, ammonia is adsorbed to produce surface H-species, including ZNH_3, ZNH_2, ZNH, and ZH; and second, surface species transform to H_2. If the first step is fast and the second step slow (i.e., (*or*)), then hydrogen production will depend on the concentration of surface species. We consider that this is the case for Fe and CoFe, where a counterclockwise trend in the hydrogen petal was observed. For the same NH_3 gas concentration, both before/after the concentration maximum, there will be greater surface H-species on the upper branch of the product petal (later in the pulse). As a result, the H_2 formation rate is higher even though the gas concentration is the same. An average apparent rate constant of hydrogen production may be estimated from the slope of a line drawn through the center of the petal,[b] 1.43 × 106/s. Hydrogen production is greater after the maximum in ammonia concentration. This corresponds to the descending branch (III and IV) in Figure 4A where the rate of ammonia conversion becomes independent of the concentration and is extinguished. Nitrogen formation (exit flux) was observed on Fe, but the signal was too low for rate calculation via Y-Procedure. This arises from the amplification of high-frequency noise in the Fourier domain solution and represents a limitation to enabling the RC petal method. Methods are currently being developed to mitigate the impact of noise in RC petal analysis.

3.5.2.2 *CoFe Bimetallic Sample*

Hydrogen production for the CoFe sample, as shown in Figure 4E, also shows a counterclockwise trend, but the petal is narrow indicating that the rate of hydrogen generation is more dependent on the ammonia gas concentration than on surface species. The apparent rate of hydrogen formation can be taken as the slope through the concentration maximum, 5.7 × 108/s.

The RC petal for nitrogen formed over CoFe is also counterclockwise, but the rate does not materialize until the ammonia gas concentration reaches a maximum. Then, the kinetic order of production rate is negative indicating that nitrogen production is inhibited by gas-phase ammonia. From this, it follows that nitrogen production is highly dependent on the surface coverage of N-containing species, while at the same time, these same N-containing species block adsorption sites for ammonia. It could be described as self-inhibition. Three dehydrogenation steps must occur before nitrogen production can proceed. Thus, nitrogen production is slower and surface hydrogen may additionally block adsorption sites.

3.5.2.3 *Co Sample*

Hydrogen production over the co catalyst was the only clockwise RC petal observed for products, as shown in Figure 4F. In this case, hydrogen production rapidly rises even at the lowest gas concentrations of ammonia in the catalyst zone. For co, the ascending branch hydrogen petal is very similar to that of ammonia. We observe direct production of H_2 withNH_3 adsorption, which would leave surface H-species in the balance. In the two-step argument made earlier, hydrogen production on Fe and CoFe is dependent on slow surface H-species transformation to H_2. On Co, however, hydrogen production is immediate and generally represented by either or, more likely, . The third possibility mentioned earlier for clockwise product petals is ; we reject this hypothesis, as the initial slope in Figure 4F is nearly 1 and not likely to represent a slow conversion to the intermediate.

The hydrogen RC petal for Co also passes through a maximum, and the rate declines even as the gas concentration is still increasing. This can be understood if adsorption sites are limited. The wide petal

[b]Apparent rate constants from different regions of the petal correspond to different coverage domains, an average apparent rate constant can be assessed from the entire petal.

shape is an indication of a state-altering experiment. The linear descending branch indicates a distinct process for hydrogen production. In this region, a slower release of H_2 now relies upon the recombination of surface H-species that remain from the initial fast hydrogen release. Thus, we can conclude that two separate processes for hydrogen formation are observed over the Co sample.

The wide petal shape for hydrogen production makes it difficult to assess an average apparent rate constant, but separate figures may be presented early (ascending branch: 1.7×10^{10}/s) and late (descending branch: 2.3×10^{8}/s) in the process. The RC petal for nitrogen production over Co, as shown in Figure 4H, shows a positive kinetic order and a counterclockwise direction indicating that nitrogen is quickly formed at low surface coverage, but also accelerates as species accumulate on the surface. Again, nitrogen can only be produced in sequence following the dehydrogenation steps and is, thus, much slower than hydrogen production. The apparent rate constant for nitrogen formation was 1.5×10^{7}/s.

3.6 Estimating Number of Active Sites

For irreversible gas adsorption, the maximum of the rate time dependence for the reactant will be observed before the maximum of the concentration time dependence. This is based on the fact that in the expression

(4)

(5)

where is the rate constant at low coverage, decreases over the course of the experiment, and the reactant petal proceeds in a clockwise direction. The rate maximum may then be used to determine the number of active sites. Again, rearranging Eqs. 4 and 5 for the first-order case of an irreversible reaction, active sites are disappearing

(6)

Then, taking the derivative

(7)

At , , hence and is still increasing, then At , and and is already decreasing, then

Then, from the regression of Eq. 7, we can determine and . At , we have and at , . Thus, by estimating from the initial slope, we can determine the number of active sites, . Following this method, the rate constant for ammonia conversion and number of active sites are calculated for each sample in Table 2 (rate constants for product generation described in the previous section are also included).

Table 2. Apparent rate constants for ammonia transformation and hydrogen, nitrogen production.[a]

catalyst active site	Fe	CoFe	Co
(ascending branch) (1/s)	4.8×10^{7}	4.2×10^{9}	3.5×10^{10}
(1/s)	1.4×10^{6}	5.7×10^{8}	1.7×10^{10} (ascending branch)
			2.3×10^{8} (descending branch)
(1/s)	0	< 0	1.5×10^{7}
active sites (sites/cm^2)	3.5×10^{8}	2.2×10^{10}	N/A

[a]Number of active sites estimate using information from ammonia adsorption over Fe and CoFe materials during ammonia pulse response experiments at 550°C.

This method for estimating active sites only applies to the case of irreversible adsorption of one reactant. We have considered ammonia adsorption to consume one active site, but dehydrogenation steps may consume additional sites. Furthermore, the release of products will regenerate free active sites. For Fe, the rate of hydrogen generation is significantly less than the rate of ammonia uptake, as shown in Figure 4, and there is limited overlap in the timing of ammonia adsorption and hydrogen release, as shown in Figure 2. For CoFe and Co, although the magnitude of the nitrogen rate may be considered negligible, the hydrogen rate on the same order as ammonia. Moreover, the timing of these uptake/release processes is similar and, hence, the active site estimation for CoFe is less-reliable overestimate. We do not report the active site estimation for Co, as the magnitude and timing of the rates are too similar.

4. CONCLUSIONS

The dynamic response of ammonia decomposing on Fe, Co, and bimetallic CoFe materials was used as a probe reaction to demonstrate the concept of a RC (rate-concentration) petal. The RC petal is a mathematical image of the kinetic pulse response experiment and can be used as a "fingerprint" for discriminating the interplay of adsorption, surface reaction, and desorption processes on different materials. From the analysis of petal shapes and directionality, we found a number of distinguishing features on these three simple materials:

Reactant rate-reactant concentration Petal —

- For all materials, the reaction rate was inhibited by the adsorption of ammonia.
- For Fe, the rate was extinguished near the concentration maximum indicating that the number of active sites was limited, estimate 3.5×10^8 sites/cm^2.
- For CoFe, the ammonia petal was symmetrical indicating more abundant sites, estimate 2.2×10^{10} sites/cm^2.
- Only Co indicated a decline in the reaction rate prior to gas concentration maximum. Extinction of the reaction rate was diminished by the regeneration of free sites through H_2 release.

Product rate-reactant concentration Petal —

- Fe and CoFe demonstrated counterclockwise petal shapes for H_2 formation indicating the control of slow surface reactions.
- Co demonstrated a clockwise petal shape for H_2 with fast hydrogen production in the same step as ammonia conversion. A linear return to zero following the concentration maximum represented a separate slow H_2 formation step dependent on the surface concentration.
- The N_2 petal shape for CoFe indicated self-inhibition processes where N species block the adsorption of ammonia required to accelerate N_2 formation.

From steady-state experiments reported previously, these three materials present distinct steady-state rates and conversions [17]. At the steady state, the surface concentration is determined by the gas concentration. The non-steady-state experiment decouples this dependence. The evolution of the rate in response to a pressure transient offers significantly greater information for how these materials regulate surface species differently. From RC petal analysis, we have demonstrated the derivation of chemico-physical insight for how simple materials orchestrate the ammonia decomposition reaction. In the future, these methods will be demonstrated with other probe reactions (e.g., oxidations) and on the complex, multicomponent industrial catalyst (direct from an operating environment). Ultimately, the RC petal examines the time dependence of the rate together with the concentration and tells the story of the interplay of adsorption, surface reaction, and product formation processes. The ability to distinguish industrial materials with such detail is enormously insightful for understanding how and why desired behavior arises at the global level.

SUPPORTING INFORMATION

The Supporting Information is available free of charge on the ACS Publications website at DOI: 10.1021/acs.jpca.9b05911:

Time dependence of the gas concentration determined for NH_3 and products (H_2 and N_2) when NH_3 is pulsed over Fe, CoFe, and Co at 550°C.

NOTES

The authors declare no competing financial interest.

ACKNOWLEDGEMENTS

This work was supported by U.S. Department of Energy (DOE), Office of Energy Efficiency and Renewable Energy (EERE), Advanced Manufacturing Office Next Generation Research and Development Projects under DOE contract no. DE-AC07-05ID14517. Accordingly, the U.S. Government retains and the publisher, by accepting the article for publication, acknowledges that the U.S. Government retains a nonexclusive, paid-up, irrevocable, world-wide license to publish or reproduce the published form of this manuscript, or allow others to do so, for U.S. Government purposes.

REFERENCES

1. Marin, G. B.; Yablonsky, G. S.; Constales, D. (2019). *Kinetics of Chemical Reactions: Decoding Complexity*; Wiley-VCH.
2. Murzin, D.; Salmi, T. (2005). *Catalytic Kinetics*; Elsevier: Amsterdam.
3. Masel, R. I. (1996). *Principles of Adsorption and Reaction on Solid Surfaces*, *Vol. 3*; John Wiley and Sons, Inc.: NY.
4. Vannice, M. A.; Joyce, W. H. (2005). *Kinetics of Catalytic Reactions*, *Vol. 134*; Springer.
5. Hinshelwood, C. N. (1926). *Kinetics of Chemical Change in Gaseous Systems*; Clarendon: Oxford.
6. Hinshelwood, C. N. (1940). *Kinetics of Chemical Change, 4th ed.*; Oxford Press: Oxford.
7. Hougen, O. A.; Watson, K. M. (1947). *Chemical Process Principles-Part 3: Kinetic and Catalysis*; John Wiley and Sons, Inc.: NY.
8. Armenise, S.; Garcia-Bordeje, E.; Valverde, J.; Romeo, E.; Monzon, A. (2013). "A Langmuir−Hinshelwood approach to the kinetic modelling of catalytic ammonia decomposition in an integral reactor," *Phys. Chem. Chem. Phys.* 15: 12104–12117.
9. Stoltze, P.; Nørskov, J. (1988). "An interpretation of the high-pressure kinetics of ammonia synthesis based on a microscopic model," *J. Catal.* 110: 1–10.
10. Gleaves, J. T.; Ebner, J. R.; Kuechler, T. C. (1988). "Temporal analysis of products (TAP)—A unique catalyst evaluation system with sub-millisecond time resolution," *Catal. Rev. Sci. Eng.* 30: 49–116.
11. Morgan, K.; Maguire, N.; Fushimi, R.; Gleaves, J.; Goguet, A.; Harold, M.; Kondratenko, E.; Menon, U.; Schuurman, Y.; Yablonsky, G. (2017). "Forty years of temporal analysis of products," *Catal. Sci. Technol.* 7: 2416–2439.
12. Redekop, E. A.; Yablonsky, G. S.; Constales, D.; Ramachandran, P. A.; Pherigo, C.; Gleaves, J. T. (2011). "The Y-Procedure methodology for the interpretation of transient kinetic data: Analysis of

irreversible adsorption," *Chem. Eng. Sci.* 66: 6441–6452.

13. Yablonsky, G. S.; Constales, D.; Shekhtman, S. O.; Gleaves, J. T. (2007). "The Y-procedure: How to extract the chemical transformation rate from reaction−diffusion data with no assumption on the kinetic model," *Chem. Eng. Sci.* 62: 6754–6767.
14. Kunz, R.; Redekop, E. A.; Borders, T.; Wang, L.; Yablonsky, G. S.; Fushimi, R. Pulse Response Analysis Using the Y-Procedure Computational Method. Chem. Eng. Sci. 2018, 192, 46–60.
15. Redekop, E. A.; Yablonsky, G. S.; Galvita, V. V.; Constales, D.; Fushimi, R.; Gleaves, J. T.; Marin, G. B. (2013). "Momentary Equilibrium (ME) in transient kinetics and its application for estimating the concentration of catalytic sites," *Ind. Eng. Chem. Res.* 52: 15417–15427.
16. Redekop, E. A.; Yablonsky, G. S.; Constales, D.; Ramachandran, P. A.; Gleaves, J. T.; Marin, G. B. (2014). "Elucidating complex catalytic mechanisms based on transient pulse-response kinetic data," *Chem. Eng. Sci.* 110: 20–30.
17. Wang, Y.; Kunz, M. R.; Siebers, S.; Rollins, H.; Gleaves, J.; Yablonsky, G.; Fushimi, R. (2019). "Transient kinetic experiments within the high conversion domain: The case of ammonia decomposition," *Catalysts* 9, No. 104.
18. Shekhtman, S. O.; Yablonsky, G. S.; Chen, S.; Gleaves, J. T. (1999). "Thin-zone TAP-reactor - Theory and application," *Chem. Eng. Sci.* 54: 4371–4378.
19. Hill, C. G.; Root, T. W. (2014). *An Introduction to Chemical Engineering Kinetics & Reactor Design, 2nd ed.*; Wiley.
20. Shekhtman, S. O.; Yablonsky, G. S. (2005). "Thin-zone TAP reactor versus differential PFR: Analysis of concentration non-uniformity for gas-solid systems," *Ind. Eng. Chem. Res.* 44: 6518–6522.
21. Shekhtman, S. O.; Yablonsky, G. S.; Gleaves, J. T.; Fushimi, R. (2003). "'State-defining' experiment in chemical kinetics—primary characterization of catalyst activity in a TAP experiment," *Chem. Eng. Sci.* 58: 4843–4859.
22. Gleaves, J. T.; Yablonskii, G. S.; Phanawadee, P.; Schuurman, Y. (1997). "TAP-2: An interrogative kinetics approach," *Appl. Catal. A* 160: 55–88.